

See discussions, stats, and author profiles for this publication at: <https://www.researchgate.net/publication/230648423>

Reactions of Lanthanide Cations with Methanol Clusters

ARTICLE *in* THE JOURNAL OF PHYSICAL CHEMISTRY A · FEBRUARY 1998

Impact Factor: 2.69 · DOI: 10.1021/jp980151c

CITATIONS

15

READS

13

2 AUTHORS:



Wenyun Lu

Princeton University

83 PUBLICATIONS 2,416 CITATIONS

SEE PROFILE



Shihe Yang

The Hong Kong University of Science and Tec...

381 PUBLICATIONS 11,332 CITATIONS

SEE PROFILE

Reactions of Lanthanide Cations with Methanol Clusters

Wenyun Lu and Shihe Yang*

Department of Chemistry, Hong Kong University of Science & Technology, Clear Water Bay, Kowloon, Hong Kong

Received: November 11, 1997; In Final Form: January 5, 1998

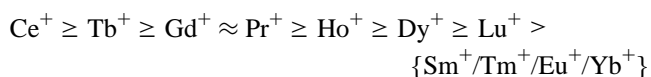
Reactions between lanthanide cations (from La^+ to Lu^+ except Pm^+) and methanol clusters were studied in a pick-up source, and the product ions were analyzed using a reflectron time-of-flight mass spectrometer (RTOFMS). Those reactive ions including La^+ , Ce^+ , Pr^+ , Nd^+ , Gd^+ , Tb^+ , Ho^+ , Er^+ , and Lu^+ react with methanol molecules forming dehydrogenation products LnCH_2O^+ and LnCH_3O^+ . For large clusters, the dehydrogenation products become $\text{Ln}(\text{OCH}_3)_2(\text{CH}_3\text{OH})_{n-2}^+$. On the contrary, the relatively unreactive lanthanide ions including Sm^+ , Eu^+ , Dy^+ , Tm^+ , and Yb^+ do not react with the methanol molecules. Only when they are solvated by a sufficient number of methanol molecules does dehydrogenation occur and yield $\text{Ln}(\text{OCH}_3)_2^+(\text{CH}_3\text{OH})_{n-2}$ ($\text{LnOCH}_3^+(\text{CH}_3\text{OH})_{n-1}$ for Eu^+). The relative reactivities of these ions are discussed in terms of their electronic configurations. Reactions of LnO^+ with methanol clusters lead to water elimination and produce $\text{LnO}_2\text{C}_2\text{H}_6(\text{CH}_3\text{OH})_{n-2}^+$. As cluster size increases to $n \approx 13$, the reaction is quenched, and only the association products $\text{LnO}(\text{CH}_3\text{OH})_n^+$ are formed.

1. Introduction

Compounds containing lanthanide elements are widely used in many areas of modern technology.¹ The unusual properties imbued by the lanthanide elements have benefited areas as diverse as heterogeneous and homogeneous catalysis, superconductivity, or advanced materials for optical, electronics, magnetic, and biomedical applications. In parallel, the organometallic chemistry of lanthanide elements has been developed as a fascinating research topic.² As catalysts or catalyst promoters, the 4f elements exhibit remarkable activity and selectivity in many processes, such as methane oxidative coupling,³ polymerization of olefins,⁴ and petroleum cracking.⁵ A variety of organolanthanide complexes can be used as efficient and selective catalysts in synthetic organic chemistry.⁶ In addition, the development of highly volatile organolanthanide complexes useful for chemical vapor deposition has been actively pursued.⁷

The gas-phase chemistry of the lanthanide cations has attracted increasing attention in recent years.^{8–19} Huang et al. first investigated the reaction between Y^+ and La^+ and alkanes with Fourier transform mass spectrometry in 1987.⁸ This was followed by the study on the reactions of Pr^+ , Eu^+ , and Gd^+ with hydrocarbons including alkanes, cycloalkanes, and alkenes.⁹ These early studies were concerned with the reactions of a few rare earth ions such as La^+ , Y^+ , Sc^+ , and Lu^+ . Only during the past several years have there been several investigations focused on the gas-phase reactions for the whole lanthanide family. These include the study of the reactions of lanthanide ions with 1,3,5-tri-*tert*-butylbenzene,¹³ hydrocarbons, for example, linear, branched, and cyclic alkanes, cyclopropane, and alkenes,¹⁵ and cyclohexacarbons $\text{C}_6\text{H}_{6+2n}$.¹⁹ These efforts allowed a comparison of the lanthanides' reactivities across the periodic table. It turns out that, whereas condensed-phase organolanthanide chemistry is similar across the series, substantial differences exist in the corresponding gas-phase Ln^+

chemistry. As an example, the reactions between Ln^+ and C_6H_{10} show the following reactivity order:¹⁹



The last four Ln^+ in the series did not react in the measurements. These distinctions were explained by their ground state electronic configurations (typically $6s^1 4f^n[\text{Xe}]$) and the variations in the energy required to promote a nonbonding 4f electron to a reactive 5d or 6s orbital. The gas-phase reactions of Ln^+ with other substrates such as fluorocarbon (refs 16, 18) and alcohols including methanol (ref 12, 17) have been reported as well. The reactions of methanol with Sc^+ , Y^+ , and Lu^+ were studied using Fourier transform mass spectrometry.¹² The metal ions undergo a dehydrogenation reaction with methanol and give product ions $\text{M}(\text{OCH}_3)_2(\text{CH}_3\text{OH})_n^+$ ($n = 0-3$). Many other products were also observed.

All the studies mentioned above were focused on the reactions of Ln^+ with single molecular substrates. It is necessary to examine their reactions under a cluster environment to see whether the reactivities of these Ln^+ are enhanced or inhibited by solvation. Thus, we studied the gas-phase chemistry of all the 14 lanthanide ions from La^+ to Lu^+ except Pm^+ with methanol clusters using the "pick-up" technique. Although there has been one report concerning the reaction of rare earth cations with methanol in the gas phase,¹² the metal ions investigated are limited to Y^+ , Sc^+ , and Lu^+ , and the reactions are with the methanol molecules. It is hoped that our work can unravel the reaction patterns of lanthanide ions with gas-phase methanol clusters as well as the relationship between the electronic structures of the metal cations and their reactivities.

2. Experimental Section

Details of the apparatus for the experiment were given previously.²⁰ Briefly, the reactions between lanthanide ions and methanol clusters were conducted using the pick-up technique,

* Corresponding author. E-mail: chsyang@usthk.ust.hk.

and the products were analyzed by a reflectron time-of-flight mass spectrometer (RTOFMS). Lanthanide oxides were mounted on the sample load lock, which was placed 9 mm downstream from a pulsed valve. The pulsed valve was used to generate the methanol cluster beam by supersonic expansion of a methanol/He gas mixture with a back-pressure of 7 atm through a 0.5-mm nozzle. The XeCl excimer laser beam was weakly focused on the sample with a power of $5 \times 10^7 \text{ W/cm}^2$. The laser-vaporized metal ions perpendicularly crossed the gas-expansion axis 10 mm from the ablation target where they were picked up by the methanol clusters, and reactions took place. The products were carried by the He gas stream and were collimated with a 1-mm skimmer. The product cations were extracted by the pulsed high voltage (950 V) and detected by the RTOFMS.

The gas mixture of methanol/He was formed by bubbling the helium gas at a pressure of 7 atm through a methanol liquid reservoir. An HPLC-grade methanol sample was obtained from Fisher Scientific. Experiments were also performed with the deuterium-substituted samples, CH_3OD (Aldrich, 99.5+ at. % D), CD_3OH (RDH, 99 at. % D), and CD_3OD (ACROS, 100 at. % D). All the samples were used without further purification. For the deuterated samples, a possible problem is the quick D/H exchange with the residual hydrogen species present in the nozzle system. Great care was taken to avoid contamination when loading these samples to the reservoir. The transfers of these samples were conducted under a helium atmosphere within an AtmosBag (Aldrich).

The ion kinetic energy measurement was carried out using a "time-of-flight" setup described in ref 20b. The laser energy and the focusing condition were kept the same as those in the reaction experiments. The ions produced by laser ablation traveled toward the ion-extraction plates. When the ions reached the center of the ion extractor, a pulsed high voltage was applied to the plates, and the ions were directed by the electric field and detected by the RTOFMS. By monitoring the ion signal intensity while scanning the delay between the laser pulse and the ion-extraction pulse, the ion kinetic energy distributions were obtained. In general, laser ablation of lanthanide oxides produced lanthanide ions Ln^+ and/or their monoxide ions LnO^+ with a kinetic energy distribution ranging from 2 to 20 eV and peaking at $\sim 6 \text{ eV}$ under our experimental conditions.

3. Results

Laser-ablation of the lanthanide oxide targets produces two kinds of ionic species under our experimental conditions, the singly charged metal cations Ln^+ and their monoxide cations LnO^+ . The production of LnO^+ species is thought to be related to the extraordinarily large bond-dissociation energies of the Ln^+-O bonds. For example, the binding energy of La^+-O is as large as 847 kJ/mol.²¹ The LaO^+ signal is even more intense than that of La^+ . For Ce, Pr, Nd, Gd, and Tb, the intensities of LnO^+ are also larger than those of the metal ions Ln^+ . The Ln^+-O bond dissociation energies for these metals are all above 700 kJ/mol. For Sm, Eu, Dy, Ho, Er, Lu, Tm, and Yb, the intensities of the metal ions Ln^+ are larger than those of the lanthanide oxide ions LnO^+ . The corresponding Ln^+-O bond dissociation energies range from 389 kJ/mol (Eu^+-O) to 598 kJ/mol (Ho^+-O). Thus, there is qualitatively a good correlation between the LnO^+ ion signal intensities and their Ln^+-O bond dissociation energies.

A general reaction pattern between Ln^+ and methanol clusters is dehydrogenation in which Ln^+ tends to attain its favorite oxidation states Ln^{3+} or Ln^{2+} . For different lanthanide ions,

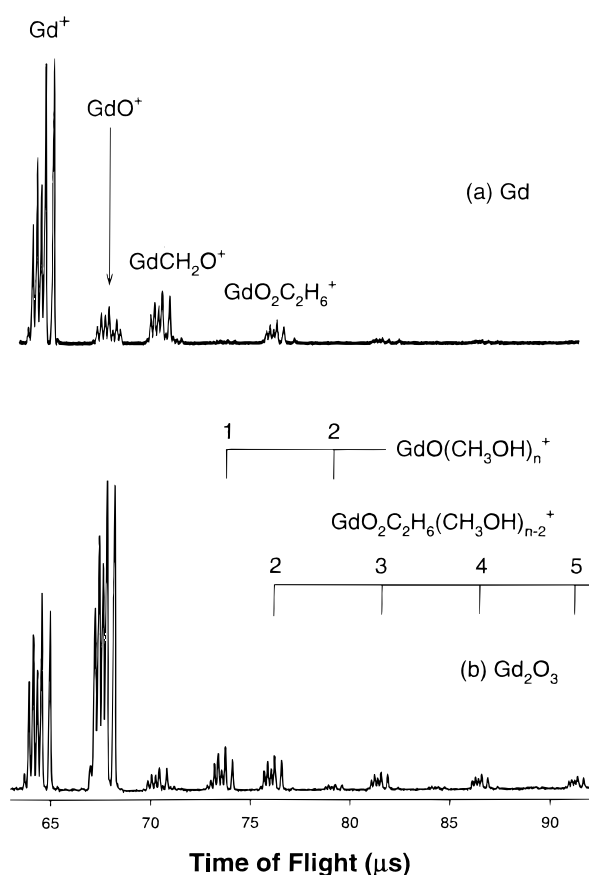


Figure 1. Mass spectra showing the product ions from the reactions of Gd^+ and GdO^+ with methanol clusters. The laser-ablation targets used are (a) Gd; (b) Gd_2O_3 .

their reactivity was found to change irregularly across the periodic table. Generally, they can be classified into two categories. La^+ , Ce^+ , Pr^+ , Nd^+ , Gd^+ , Tb^+ , Ho^+ , Er^+ , and Lu^+ belong to the first category. They can react with single methanol molecules to form dehydrogenation products LnCH_2O^+ and LnCH_3O^+ in addition to the normal association products $\text{Ln}(\text{CH}_3\text{OH})_n^+$. The remaining five lanthanide ions, Sm^+ , Eu^+ , Dy^+ , Tm^+ , and Yb^+ , cannot initiate dehydrogenation of methanol molecules. Only association products $\text{Ln}(\text{CH}_3\text{OH})_n^+$ were formed. Interestingly, it was found that although these relatively unreactive lanthanide ions cannot react with a single methanol, the dehydrogenation reactions readily occur for their methanol cluster ions $\text{Ln}^+(\text{CH}_3\text{OH})_n$ leading to $\text{LnO}_2\text{C}_2\text{H}_6(\text{CH}_3\text{OH})_{n-2}^+$ products when the clusters reach certain sizes.

3.1. Gadolinium (Gd). We used both Gd_2O_3 powder and Gd metal to produce Gd^+ . When using Gd_2O_3 , both Gd^+ and GdO^+ ions were observed. The intensity of GdO^+ ions is even larger than that of Gd^+ ions. When using Gd metal, besides the Gd^+ ion signal, GdO^+ was also observed although it is much smaller. These oxide species are likely to come from the quick oxidation of the Gd metal as the binding energy of $\text{Gd}-\text{O}$ is very large. The difference in the relative abundance of Gd^+ and GdO^+ from laser ablation of Gd and Gd_2O_3 allows us to distinguish between the products from reactions of Gd^+ and those from reactions of GdO^+ with methanol clusters.

Figure 1a shows the mass spectrum of reaction products from the reaction of methanol clusters and ionic species produced by laser ablation of Gd. Five major isotopes of Gd can be clearly identified.²² One can see that the intensity of GdO^+ is quite small compared with that of Gd^+ . The majority of the

product ions observed comes from the reaction between Gd^+ and the methanol clusters $(\text{CH}_3\text{OH})_n$. At the flight time around $70 \mu\text{s}$, there are several peaks with one mass difference. Careful analysis of these peaks shows that the major signals correspond to GdCH_2O^+ with smaller amounts of GdCH_3O^+ and GdCH_3OH^+ . The corresponding intensity ratio of these three ions is 85.2:9.9:4.9. For larger clusters, $\text{GdO}_2\text{C}_2\text{H}_6^+$ ions were observed with a smaller intensity than that of GdCH_2O^+ . They are likely to be from the dehydrogenation reaction of $\text{Gd}(\text{CH}_3\text{OH})_2^+$. Deuteration experiments using CH_3OD and CD_3OH established that the two lost hydrogen atoms are from the OH groups in the methanol molecules. Thus the reaction products $\text{GdO}_2\text{C}_2\text{H}_6^+$ may correspond to $\text{Gd}(\text{OCH}_3)_2^+$ in which Gd obtains its favorite oxidation state of +3. For even larger clusters, $\text{GdO}_2\text{C}_2\text{H}_6(\text{CH}_3\text{OH})_{n-2}^+$ ions were observed but with much smaller intensities.

Figure 1b shows the same mass spectrum as in Figure 1a except that in this case Gd_2O_3 is used as the ablation target. The intensity of GdO^+ is found to be much larger than that of Gd^+ . Thus we need to consider possible reactions of GdO^+ . The $\text{GdO}(\text{CH}_3\text{OH})_n^+$ ion signals are readily ascribed to the association products of GdO^+ and $(\text{CH}_3\text{OH})_n$. Other product ions include GdCH_2O^+ and $\text{GdO}_2\text{C}_2\text{H}_6(\text{CH}_3\text{OH})_{n-2}^+$ ($n \geq 2$). Clearly, the GdCH_2O^+ ions are from the reaction of Gd^+ with methanol molecules. The question is the origin of $\text{GdO}_2\text{C}_2\text{H}_6^+$. As can be seen from Figure 1b, the intensity of $\text{GdO}_2\text{C}_2\text{H}_6^+$ is larger than that of GdCH_2O^+ in contrast to what is observed in Figure 1a for the reaction of Gd^+ . The higher intensity of $\text{GdO}_2\text{C}_2\text{H}_6^+$ in Figure 1b then indicates that they contain the contributions from the reaction of GdO^+ . Similar patterns were observed in a previous FTICR study on the reactions of ScO^+ , YO^+ , and LuO^+ with methanol.¹² The detailed structure of $\text{GdO}_2\text{C}_2\text{H}_6^+$ is unclear at present, but it is expected to be from $\text{GdO}(\text{CH}_3\text{OH})_2^+$ with the loss of one water molecule. For larger cluster ions $\text{GdO}_2\text{C}_2\text{H}_6(\text{CH}_3\text{OH})_{n-2}^+$, we believe that they also contain significant contributions from the reactions of $\text{GdO}(\text{CH}_3\text{OH})_n^+$ besides the contributions from $\text{Gd}(\text{CH}_3\text{OH})_n^+$.

3.2. La^+ , Pr^+ , Ce^+ , Nd^+ , Tb^+ , and Er^+ . Figure 2a shows the mass spectrum of the ions from laser ablation of La_2O_3 with pure He expansion. Both La^+ and LaO^+ ions were detected, and the ion intensity of LaO^+ is even larger than that of La^+ . When using the methanol/He gas mixture for the expansion, additional ion signals were observed resulting from the reactions between La^+ , LaO^+ , and the methanol clusters as shown in Figure 2b. The two small peaks at a flight time of around $66 \mu\text{s}$ correspond to LaCH_2O^+ and LaCH_3O^+ , respectively. The association product $\text{La}(\text{CH}_3\text{OH})^+$ from La^+ can also be identified on the right of the LaCH_3O^+ peak but with a much smaller intensity. It appears that the reaction between La^+ with CH_3OH molecules mainly produces the dehydrogenation products LaCH_2O^+ and LaCH_3O^+ . In the large-mass region, two series of cluster ions were identified; a_n corresponds to $\text{LaO}_2\text{C}_2\text{H}_6(\text{CH}_3\text{OH})_{n-2}^+$ and b_n corresponds to the association products $\text{LaO}(\text{CH}_3\text{OH})_n^+$ from LaO^+ . The intensities for both series decrease with increasing cluster size with the former being the predominant one.

To ascertain the mass assignment, experiments were performed using deuterium-substituted methanol samples. The results are given in Table 1. For $n = 1$, the major products are LaCH_2O^+ and LaCH_3O^+ . The deuterium substitution experiments also confirm our assignments for the a_n series in Figure 2b corresponding to $\text{LaO}_2\text{C}_2\text{H}_6(\text{CH}_3\text{OH})_{n-2}^+$ and not $\text{LaCH}_2\text{O}^+(\text{CH}_3\text{OH})_{n-1}$. Similar to the situation of Gd^+ , we suspect that the cluster ions $\text{LaO}_2\text{C}_2\text{H}_6(\text{CH}_3\text{OH})_{n-2}^+$ contain the

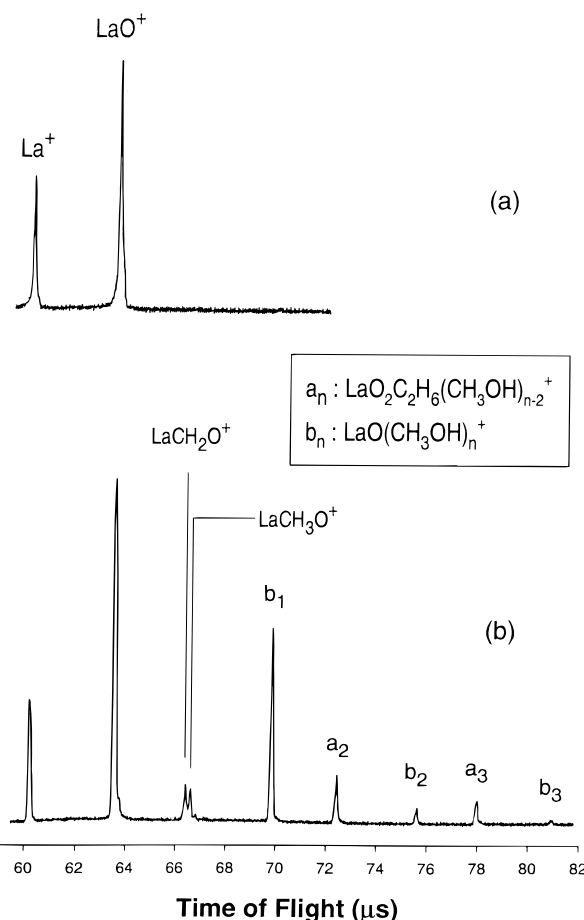


Figure 2. Mass spectra showing the product ions observed when La_2O_3 is used as the target: (a) ions observed with pure He expansion; (b) product ions observed with methanol/He expansion.

TABLE 1: Product Ions Observed from the Reactions of La^+ and LaO^+ with Methanol Clusters

methanol	ion mass	assignment
CH_3OH	169	LaCH_2O^+
	170	LaCH_3O^+
	171	LaCH_3OH^+
	201, 233, ...	$\text{LaO}_2\text{C}_2\text{H}_6(\text{CH}_3\text{OH})_{n-2}^+, n = 2, 3, \dots$
	187, 219, 251, ...	$\text{LaO}(\text{CH}_3\text{OH})_n^+, n = 1, 2, 3, \dots$
CH_3OD	169	LaCH_2O^+
	170	LaCH_3O^+
	172	LaCH_3OD^+
	201, 234, ...	$\text{LaO}_2\text{C}_2\text{H}_6(\text{CH}_3\text{OD})_{n-2}^+, n = 2, 3, \dots$
	188, 221, 254, ...	$\text{LaO}(\text{CH}_3\text{OD})_n^+, n = 1, 2, 3, \dots$
CD_3OH	171	LaCD_2O^+
	173	LaCD_3O^+
	174	LaCD_3OH^+
	207, 242, ...	$\text{LaO}_2\text{C}_2\text{D}_6(\text{CD}_3\text{OH})_{n-2}^+, n = 2, 3, \dots$
	190, 225, 264, ...	$\text{LaO}(\text{CD}_3\text{OH})_n^+, n = 1, 2, 3, \dots$
CD_3OD	171	LaCD_2O^+
	173	LaCD_3O^+
	175	LaCD_3OH^+
	207, 243, ...	$\text{LaO}_2\text{C}_2\text{D}_6(\text{CD}_3\text{OD})_{n-2}^+, n = 2, 3, \dots$
	191, 227, 263, ...	$\text{LaO}(\text{CD}_3\text{OD})_n^+, n = 1, 2, 3, \dots$

contributions from the reaction of both $\text{La}(\text{CH}_3\text{OH})_n^+$ and $\text{LaO}(\text{CH}_3\text{OH})_n^+$. Considering that the intensity of LaO^+ is much larger than that of La^+ , the contributions from the reactions of $\text{LaO}(\text{CH}_3\text{OH})_n^+$ are expected to be much larger than that from $\text{La}(\text{CH}_3\text{OH})_n^+$.

Figure 3a shows the mass spectrum for clusters containing 9–17 methanol molecules. In this region, the intensity of $\text{LaO}_2\text{C}_2\text{H}_6(\text{CH}_3\text{OH})_{n-2}^+$ decreases quickly (from ref 20a), and

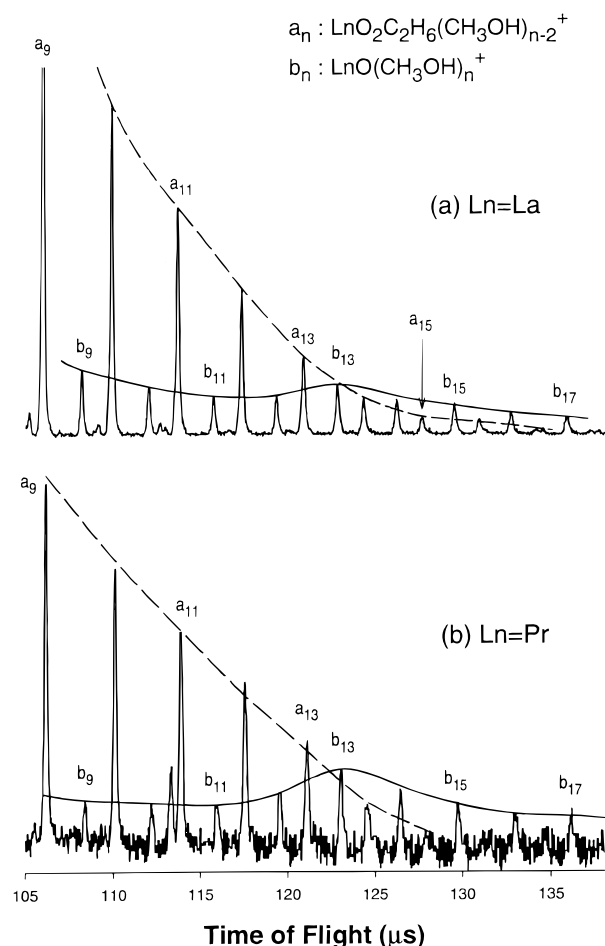


Figure 3. Mass spectra showing the intensity shift from $\text{LaO}_2\text{C}_2\text{H}_6(\text{CH}_3\text{OH})_{n-2}^+$ to $\text{LnO}(\text{CH}_3\text{OH})_n^+$ in the large-cluster-size region: (a) $\text{Ln} = \text{La}$; (b) $\text{Ln} = \text{Pr}$.

it drops to near zero for $n = 17$. On the other hand, the intensity of $\text{LaO}(\text{CH}_3\text{OH})_n^+$ shows irregular behavior with increasing cluster size; there is an increase around $n = 12$, followed by a smooth decrease, and its intensity overtakes that of $\text{LaO}_2\text{C}_2\text{H}_6(\text{CH}_3\text{OH})_{n-2}^+$ with the same n . One possible explanation for this intensity switch is that the reaction products may originate from the dehydration reactions that were found to occur in alkali metal ion–methanol clusters $\text{M}^+(\text{CH}_3\text{OH})_n$ ($\text{M} = \text{Li}, \text{Na}, \text{K}, \text{Rb}, \text{Cs}$).^{23–25} In such an intracluster dehydration reaction, the positive charge simply acts to lower the activation barrier for the reaction beyond the first solvation shell. Considering that $\text{LaO}(\text{CH}_3\text{OH})_n^+$ has the same mass as $\text{LaO}_2\text{C}_2\text{H}_6(\text{CH}_3\text{OH})_{n-2}(\text{H}_2\text{O})^+$, the dehydration products from $\text{LaO}_2\text{C}_2\text{H}_6(\text{CH}_3\text{OH})_n^+$ would lead to the increase of the intensity of $\text{LaO}(\text{CH}_3\text{OH})_n^+$. This assumption can be tested by a deuterium-substitution experiment. Due to the greater stabilization of deuterated methanol systems than of the CH_3OH -containing systems,²⁶ the dehydration of metal ion–methanol clusters is expected to be less favorable for $\text{M}^+(\text{CD}_3\text{OD})_n$ than for $\text{M}^+(\text{CH}_3\text{OH})_n$. This should be reflected by the ratio of the intensity of the product $\text{M}^+(\text{methanol})_n(\text{water})$ to that of its parent $\text{M}^+(\text{methanol})_{n+2}$. The ratio for the CD_3OD system was found to be several times smaller than that for CH_3OH system at a fixed n in reactions with Cs^+ and Fe^+ .²³ Our results are depicted in Figure 4. It appears that there is no obvious difference in the product/reactant ratio for different methanol systems. We conclude that the increase of the intensity of $\text{LaO}(\text{CH}_3\text{OH})_n^+$ is not from the dehydration reaction of $\text{LaO}_2\text{C}_2\text{H}_6(\text{CH}_3\text{OH})_n^+$. Another explanation assumes that the

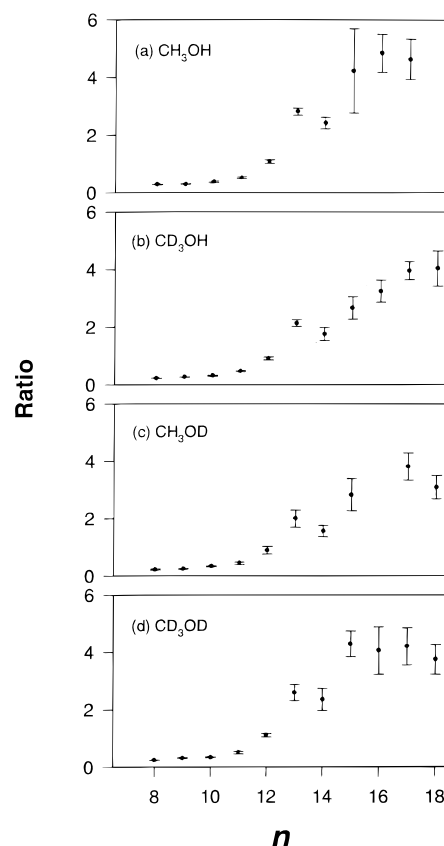


Figure 4. Intensity ratios between $\text{LaO}(\text{methanol})_n^+$ and $\text{LaO}_2\text{C}_2\text{H}_6(\text{D})_6(\text{methanol})_n^+$ for different deuterium-substituted methanol molecules: (a) CH_3OH ; (b) CD_3OH ; (c) CH_3OD ; (d) CD_3OD . Error bars represent $\pm\sigma$ of 10 mass spectra.

reaction of $\text{LaO}(\text{CH}_3\text{OH})_n^+$ to give $\text{LaO}_2\text{C}_2\text{H}_6(\text{CH}_3\text{OH})_{n-2}^+$ is quenched at a large cluster size. This may be due to the difficulty in removing the water product in a large cluster environment. Thus the decrease of the $\text{LaO}_2\text{C}_2\text{H}_6(\text{CH}_3\text{OH})_{n-2}^+$ ion signal corresponds to the increase of the $\text{LaO}(\text{CH}_3\text{OH})_n^+$ signals with the increasing cluster size.

The metal ions Pr^+ , Ce^+ , Nd^+ , Tb^+ , and Er^+ and their oxides exhibit similar product patterns to those of Gd^+ and La^+ and their oxides upon reaction with methanol molecules. For example, the reaction of Pr^+ with methanol molecules gives PrCH_2O^+ , PrCH_3O^+ , and PrCH_3OH^+ . For the reactions of Pr^+ and PrO^+ with small methanol clusters, the products are $\text{PrO}_2\text{C}_2\text{H}_6(\text{CH}_3\text{OH})_{n-2}^+$. Analogous to the case of LaO^+ , the intensity shifts to $\text{PrO}(\text{CH}_3\text{OH})_n^+$ from $\text{PrO}_2\text{C}_2\text{H}_6(\text{CH}_3\text{OH})_{n-2}^+$ at $n \approx 13$, as can be seen from Figure 3b. The only exception comes from Er^+ , which does not yield ErCH_3O^+ while reacting with methanol molecules.

3.3. Ho^+ , Lu^+ , Dy^+ , and Tm^+ . The association is the major channel for the reactions of Ho^+ , Lu^+ , Dy^+ , and Tm^+ with methanol molecules. A very small amount of dehydrogenation products (e.g., HoCH_2O^+) is produced. This is in striking contrast to the reaction patterns of La^+ with methanol. The difference in the product distribution reflects the different reactivity of different lanthanide ions with methanol molecules. However, they do react with methanol clusters above a certain size, as shown in Figure 5 for Ho^+ . Since the intensity of HoO^+ is much smaller than that of Ho^+ in the laser-ablation source, the products are mainly from the reaction of methanol clusters with Ho^+ . As can be seen from the spectrum, for $n = 1$, the major product is $\text{Ho}(\text{CH}_3\text{OH})^+$ with a very small amount of HoCH_2O^+ and HoCH_3O^+ . Only at $n = 2$ does a reaction start

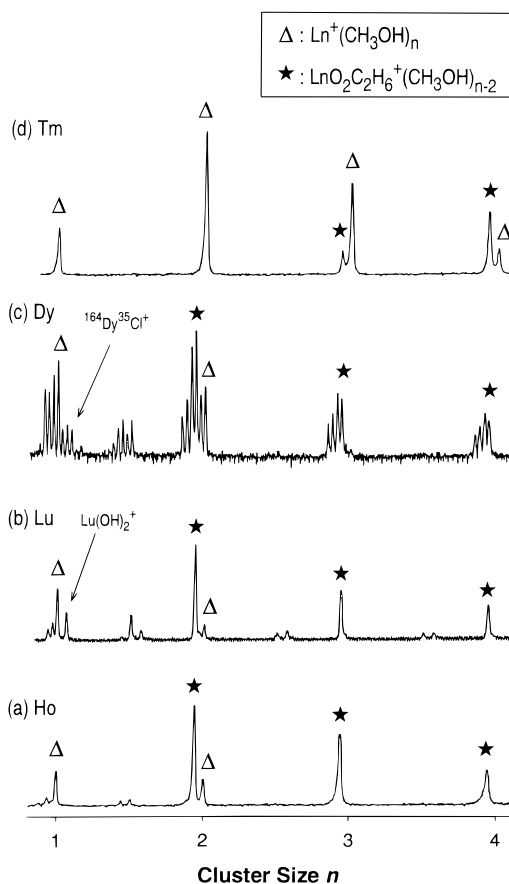


Figure 5. Mass spectra showing the product ions from the reactions between lanthanide cations and methanol clusters: (a) Ho; (b) Lu; (c) Dy; (d) Tm. For Dy, the product ions containing the most abundant ^{164}Dy isotope are labeled. The Dy_2O_3 target used contains DyCl_3 impurities. The peak labeled as $^{164}\text{DyO}_2\text{C}_2\text{H}_6^+$ contains the contributions from $^{162}\text{Dy}(\text{CH}_3\text{OH})_2^+$.

to occur for $\text{Ho}(\text{CH}_3\text{OH})_2$ to give $\text{HoO}_2\text{C}_2\text{H}_6^+$. For $n \geq 3$, no signals of $\text{Ho}(\text{CH}_3\text{OH})_n^+$ were observed. All the ions correspond to the dehydrogenation products $\text{HoO}_2\text{C}_2\text{H}_6(\text{CH}_3\text{OH})_{n-2}^+$. Lu^+ and Dy^+ show similar reaction patterns. The only thing special about Lu^+ in terms of its reaction with methanol molecules is that a significant amount of LuOH^+ ions is formed, which is not observed for other lanthanide ions. A previous study on the reaction of Lu^+ with methanol molecules using Fourier transform mass spectrometry also found a substantial amount of LuOH^+ product ions besides the dehydrogenation product LuOCH_3^+ .¹²

Tm has only one isotope, ^{169}Tm ,²² and no TmO^+ signals were observed when laser ablating its oxide Tm_2O_3 . The reaction products are exclusively from the reaction of Tm^+ with a methanol cluster $(\text{CH}_3\text{OH})_n$. The corresponding mass spectrum is shown in Figure 6d. Obviously Tm^+ is even more unreactive toward methanol than Dy^+ . For $n = 1$ and 2, only association products $\text{Tm}(\text{CH}_3\text{OH})_n$ were observed. $\text{Tm}(\text{CH}_3\text{OH})_n^+$ starts to react to give a small amount of $\text{TmO}_2\text{C}_2\text{H}_6(\text{CH}_3\text{OH})_{n-2}^+$ ions at $n = 3$. The relative intensity for the two species is about 1:4. At $n = 4$, this ratio becomes about 3:1. For larger clusters, $\text{TmO}_2\text{C}_2\text{H}_6(\text{CH}_3\text{OH})_{n-2}^+$ is still the dominant cluster ion as can be seen from Figure 6. Clusters containing as many as 18 methanol molecules can be identified although the intensity of the large cluster decreases quickly with increasing cluster size. It appears that the reaction of $\text{Tm}(\text{CH}_3\text{OH})_n^+$ to give $\text{TmO}_2\text{C}_2\text{H}_6(\text{CH}_3\text{OH})_{n-2}^+$ is not quenched at a large cluster size in contrast to that of $\text{LaO}(\text{CH}_3\text{OH})_n^+$. Besides, $\text{TmO}(\text{CH}_3\text{OH})_n^+$

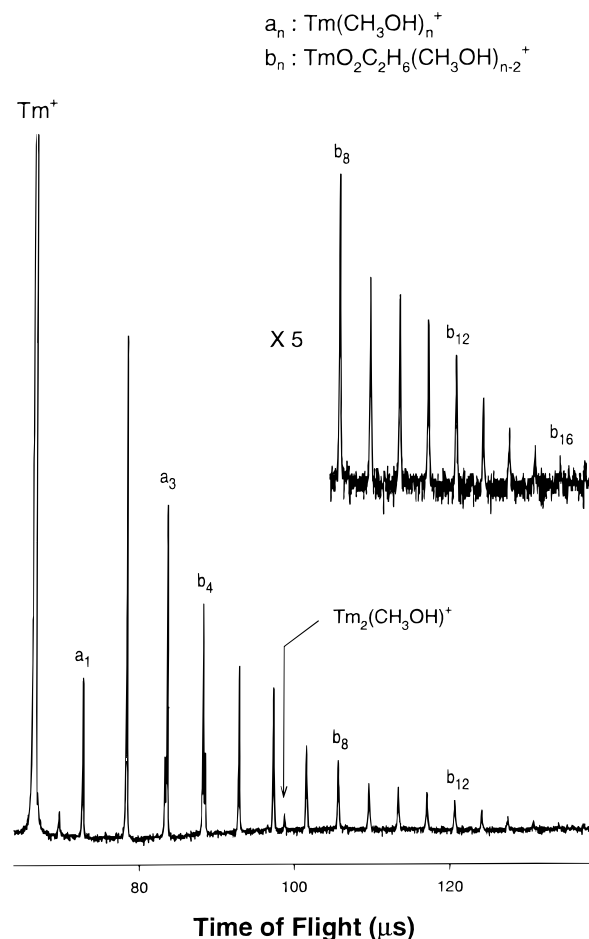


Figure 6. Overview of the mass spectrum showing the product ions from the reaction of Tm^+ with methanol clusters.

was not observed in this region. This is consistent with the fact that very few TmO^+ ions were produced when laser ablating the Tm_2O_3 target, and the observed product ions come from the reaction of Tm^+ . This serves as a support for the proposed mechanism for the intensity increase of the $\text{LaO}(\text{CH}_3\text{OH})_n^+$ cluster ion for n at 13. If the observed product ions $\text{LaO}_2\text{C}_2\text{H}_6(\text{CH}_3\text{OH})_{n-2}^+$ come from the reaction of La^+ only, it is expected that $\text{LaO}(\text{CH}_3\text{OH})_n^+$ will not be observed at a large cluster size. The increase of the $\text{LaO}(\text{CH}_3\text{OH})_n^+$ intensity for n at around 13 results from the quenching of the water-elimination reaction.

3.4. Sm^+ , Yb^+ , and Eu^+ . Laser ablation of Sm_2O_3 and Yb_2O_3 produces mainly metal cations with a small amount of their oxides. For small clusters, the association products $\text{M}(\text{CH}_3\text{OH})_n^+$ were observed for $n \leq 3$. The dehydrogenation reaction to form $\text{MO}_2\text{C}_2\text{H}_6(\text{CH}_3\text{OH})_{n-2}^+$ starts for the cluster containing four methanol molecules. For the reaction of Eu^+ with methanol clusters, association products $\text{Eu}(\text{CH}_3\text{OH})_n^+$ are formed for small clusters ($n \leq 5$) and the dehydrogenation starts at $n = 6$. In this case, however, the dehydrogenation of $\text{Eu}(\text{CH}_3\text{OH})_n^+$ involves the loss of only one hydrogen atom instead of two hydrogen atoms. This is not surprising since Eu^+ has an electronic configuration of $6s^1 4f^7$. By losing one electron to form Eu^{2+} , it forms a stable half-filled electronic configuration of $4f^7$. Thus Eu^+ may preferentially form the EuOCH_3^+ species in which its oxidation state is close to +2 in much the same way as for the alkaline earth metal ion reactions.^{20b}

To summarize, the general reaction pattern for the lanthanide cations Ln^+ with methanol clusters is the dehydrogenation reaction with the loss of one or two hydrogen atoms. With the

TABLE 2: Reaction Patterns of Lanthanide Cations Ln^+ with Methanol Clusters $(\text{CH}_3\text{OH})_n$

Ln^+	reaction start at $n =$	reaction products			
		LnCH_2O^+	LnCH_3O^+	LnCH_3OH^+	$\text{LnO}_2\text{C}_2\text{H}_6(\text{CH}_3\text{OH})_{n-2}^+$
La^+	1	✓	✓	✓	✓
Ce^+	1	✓	✓	✓	✓
Pr^+	1	✓	✓	✓	✓
Nd^+	1	✓	✓	✓	✓
Sm^+	4				✓
Eu^+	6				✓
Gd^+	1	✓	✓	✓	✓
Tb^+	1	✓		✓	✓
Dy^+	2				✓
Ho^+	1	✓	✓	✓	✓
Er^+	1	✓		✓	✓
Tm^+	3				✓
Yb^+	4				✓
Lu^+	1	✓	✓	✓	✓

single methanol molecules, this leads to the formation of LnCH_2O^+ and LnCH_3O^+ besides the normal association products LnCH_3OH^+ . For larger clusters, the dehydrogenation of the $\text{Ln}(\text{CH}_3\text{OH})_n^+$ cluster ions was observed. The resulting product ions are $\text{LnOCH}_3(\text{CH}_3\text{OH})_{n-1}^+$ (for Eu^+) and $\text{LnO}_2\text{C}_2\text{H}_6(\text{CH}_3\text{OH})_{n-2}^+$ (for other lanthanide ions).

The lanthanide ions show different reactivity in their reaction with methanol clusters. The reactive ions can react with single molecules to give dehydrogenation products. These include La^+ , Ce^+ , Pr^+ , Nd^+ , Gd^+ , Tb^+ , Ho^+ , Er^+ , and Lu^+ . The relatively unreactive ions Sm^+ , Eu^+ , Dy^+ , Tm^+ , and Yb^+ cannot react with methanol molecules to generate dehydrogenation products. Only association products were observed. However, the corresponding metal–methanol cluster ions were found to undergo dehydrogenation when the cluster reaches a certain size. The critical sizes are 4, 6, 2, 3 and 4 for Sm^+ , Eu^+ , Dy^+ , Tm^+ and Yb^+ , respectively. These observations indicate that the formation of the cluster environment thermodynamically favors the dehydrogenation products. This enhanced stability of the dehydration products with increasing cluster size stems from the increased electrostatic interactions between the metal cations and the methanol molecules; the metal atoms become triply charged in the products, whereas they were singly charged in the reactants. The overall results are summarized in Table 2. For those lanthanides whose oxide ions LnO^+ are quite abundant in the laser-ablation source, their reactions with small methanol clusters lead to the products $\text{LnO}_2\text{C}_2\text{H}_6(\text{CH}_3\text{OH})_{n-2}^+$, which have the same masses as those from the dehydrogenation of $\text{Ln}(\text{CH}_3\text{OH})_n^+$. The contributions from the former are believed to be greater than those from the latter. Besides, at larger cluster sizes, the reaction of $\text{LnO}(\text{CH}_3\text{OH})_n^+$ to give $\text{LnO}_2\text{C}_2\text{H}_6(\text{CH}_3\text{OH})_{n-2}^+$ is quenched and there is an increase of the intensity of $\text{LnO}(\text{CH}_3\text{OH})_n^+$ for n at around 13 for these lanthanide ions.

4. Discussion

4.1. Reactivity Order of Lanthanide Ions Ln^+ toward Methanol Molecules. As has been mentioned above, the lanthanide ions can be classified into two categories according to their reactivities toward methanol clusters. The first includes the Ln^+ ions that can react with single methanol molecules to give dehydrogenation products such as LnCH_2O^+ . The second refers to the relatively unreactive Ln^+ cations for which the dehydrogenation reactions start to occur only when the metal ions are solvated by a sufficient number of methanol molecules. The comparison of reactivities of the lanthanide ions belonging

TABLE 3: Product Distributions for the Reactions between Lanthanide Cations Ln^+ and Methanol Molecules

Ln^+	LnCH_2O^+ (%)	LnCH_3O^+ (%)	LnCH_3OH^+ (%)	other products
La^+	47.5	42.2	10.3	
Ce^+	63.7	31.2	5.1	
Pr^+	29.6	47.3	23.1	
Nd^+	29.5	32.5	40.0	
Gd^+	85.2	9.9	4.9	
Tb^+	76.4	0	23.6	
Ho^+	19.5	6.8	73.7	
Er^+	55.5	0	44.5	
Lu^+	14.4	22.2	63.4	LuOH^+ , $\text{Lu}(\text{H}_2\text{O})^+$

to the second category (Sm^+ , Eu^+ , Dy^+ , Tm^+ , and Yb^+) is straightforward. The less reactive metal ion would require a larger extent of methanol solvation to make the reaction occur; i.e., reaction occurs at a larger cluster size. Qualitatively there appears to be a correlation between the reactivity and the critical cluster size where the dehydrogenation reaction starts to occur. Given that the critical sizes for these ions are (see Table 2) 4, 6, 2, 3, and 4 for Sm^+ , Eu^+ , Dy^+ , Tm^+ , and Yb^+ , respectively, the following reactivity order is expected for the five metal ions: $\text{Dy}^+ > \text{Tm}^+ > [\text{Sm}^+ \sim \text{Yb}^+] > \text{Eu}^+$. The reactivities of Sm^+ and Yb^+ are close; they both start to react at $n = 4$. However, the intensity ratios between $\text{LnO}_2\text{C}_2\text{H}_6(\text{CH}_3\text{OH})_2^+$ and $\text{Ln}(\text{CH}_3\text{OH})_4^+$ are different for these two metal ions. It is 1:1.7 for Sm^+ and 1:2 for Yb^+ . Thus, the reactivity of Sm^+ seems to be slightly higher than that of Yb^+ . Summing up the above considerations, we obtain the following reactivity order: $\text{Dy}^+ > \text{Tm}^+ > \text{Sm}^+ \geq \text{Yb}^+ > \text{Eu}^+$.

Much more difficult is the derivation of the reactivity order of the lanthanide ions that can all react with methanol molecules leading to dehydrogenation. Nevertheless, we can exploit the relationship between the relative rate constants and the relative abundance of the dehydrogenation products for the reaction. Our assumption is that the larger the relative rate constants, the more the reaction products. This was revealed for the reactions between lanthanide ions and hydrocarbons.¹⁵ In our experiments, the lanthanide ions react with methanol molecules and produce $\text{Ln}(\text{CH}_3\text{OH})^+$, LnCH_3O^+ , and LaCH_2O^+ . The relative abundance for these three species is used to compare the reactivities for their reactions with methanol molecules. Table 3 summarizes the relative abundance of the three product ions observed in the mass spectra for the lanthanide ions of the first category (La^+ , Ce^+ , Pr^+ , Nd^+ , Gd^+ , Tb^+ , Ho^+ , Er^+ , and Lu^+). Among the nine lanthanide ions, Gd^+ is the most reactive as the relative abundance of the dehydrogenation product GdCH_2O^+ is the largest. Ho^+ and Lu^+ are the least reactive as the reaction products are mainly the association products $\text{Ho}(\text{CH}_3\text{OH})^+$ and $\text{Lu}(\text{CH}_3\text{OH})^+$ and few dehydrogenation products were observed. For Lu^+ , other products such as LuOH^+ are also produced. For other lanthanide ions, their reactivities are in between those of Gd^+ and Ho^+ , Lu^+ . The dehydrogenation products include LnCH_2O^+ and LnCH_3O^+ . Considering the relative abundance for the three ionic species, we obtain the following reactivity order: $\text{Gd}^+ > \text{Ce}^+ > \text{La}^+ > \text{Tb}^+ > \text{Pr}^+ > \text{Er}^+ > \text{Nd}^+ > \text{Lu}^+ \geq \text{Ho}^+$. Overall, the reactivity order is then $\text{Gd}^+ > \text{Ce}^+ > \text{La}^+ > \text{Tb}^+ > \text{Pr}^+ > \text{Er}^+ > \text{Nd}^+ > \text{Lu}^+ \geq \text{Ho}^+ > \text{Dy}^+ > \text{Tm}^+ > \text{Sm}^+ \geq \text{Yb}^+ > \text{Eu}^+$.

Such a reactivity order shares some similarity with the previous work on the reactivity of lanthanide ions with hydrocarbons.^{15,19} However, the previous work was mainly focused on the reactions with single molecules, while our method incorporates the reactions of metal ions with the molecular clusters. By comparing the different cluster sizes at

which the reactions start to occur for different Ln^+ cations, we can obtain a rough reactivity order of the Ln^+ cations for the reactions with this substrate. Together with the knowledge of the relative abundance of the products and the reactants, we can obtain a reasonable reactivity order of the Ln^+ . Although the work presented here is focused on the methanol substrate, we expect that such an approach is applicable to other substrates such as hydrocarbons.

It is important to note that the laser-ablated metal ions may not necessarily be in their ground states. While we cannot exclude possible reactions of the electronically excited-state metal ions, we believe that the observed reaction products are mainly from the ground-state reactions. Otherwise, the cluster size selectivity of the reactions would be washed out since the excited-state reactions are much more exothermic.

4.2. The Correlation between Reactivity and Electronic Structures of Ln^+ Ions. The different reactivities of Ln^+ toward methanol are likely to be related to their electronic structures. Beauchamp et al. first suggested that insertion of Ln^+ ions into a C–H or C–C bond require that Ln^+ has two non-f electrons in their ground electronic states.⁹ This is based on the fact that the 4f electrons are buried so deeply within the lanthanide ions (ref 27) that they are very inactive in the sense that covalent bonds involving the compact 4f orbital are inherently weak. For the reaction of Ln^+ with methanol species, the reactions are expected to proceed through an insertion mechanism.¹² The formation of $\text{H–Ln}^+–\text{OCH}_3$ species requires that Ln^+ has two reactive valence electrons. Since most of the Ln^+ cations have an electronic configuration of $6s^1 4f^n$, a promotion to the triplet $5d^1 6s^1 4f^{n-1}$ or $5d^2 4f^{n-1}$ configuration is needed for the insertion of Ln^+ into the O–H bond. Such a promotion from the ground state may occur before the insertion or through a curve-crossing process between the related potential energy surfaces.^{15,28} In the latter case, the two potential energy surfaces derived from the configurations with only one electron in a non-f orbital ($6s^1 4f^n$) and with two electrons in the non-f orbital ($6s^1 5d^1 4f^{n-1}$ or $5d^2 4f^{n-1}$) intersect each other along the reaction path. Thus, the energy required for the promotion from the ground state to the states with two non-f electrons may determine the relative reactivities for their reactions with methanol species. The lower the energy needed for the promotion, the higher the reactivity of Ln^+ .

Figure 7 presents the promotion energies for Ln^+ .²⁹ The x-axis corresponds to all the 14 Ln^+ ions with increasing reactivity derived above for their reactions with methanol clusters. The y-axis corresponds to the promotion energies from the ground state ($6s^1 4f^n$) to the lowest-lying state with the configurations of $6s^1 5d^1 4f^{n-1}$ and $5d^2 4f^{n-1}$. Apparently, there is a good correlation between the reactivity and the promotion energies to the $6s^1 5d^1 4f^{n-1}$ configuration. For example, the promotion energy of the least-reactive Eu^+ has a promotion energy as high as 94.2 kcal/mol. The results are in accordance with the previous studies on the reactions of Ln^+ ions with hydrocarbons.^{15,19}

While the correlation between the reactivity and the promotion energy to the configuration $5d^1 6s^1 4f^{n-1}$ state is nice, such a correlation does not seem to hold between the reactivity and the promotion energy to the configuration $5d^2 4f^{n-1}$ as seen in Figure 7. In other words, the $6s^1 5d^1 4f^{n-1}$ configuration appears to be more effective for O–H activation. From the radial distributions of 4f, 5s, 5p, 5d, 6s, and 6p orbitals of the Ln^+ ions,³⁰ 5d is external with respect to 4f and internal with respect to 6s and 6p. Thus the Ln^+ with an electronic configuration of $5d^2 4f^{n-1}$ may not be able to form two very effective covalent

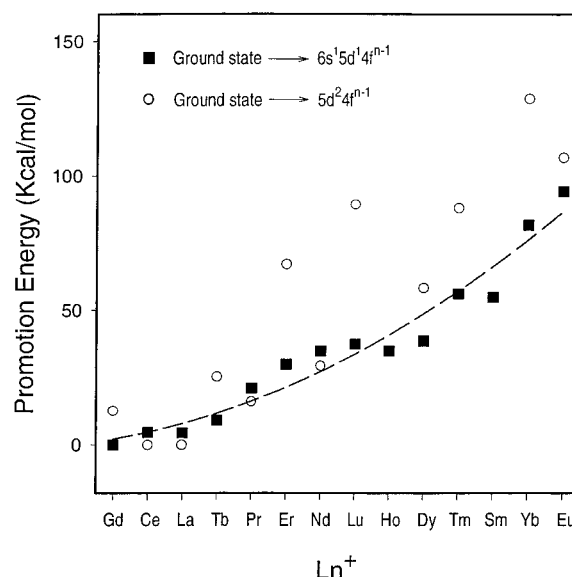


Figure 7. Relative reactivity vs the promotion energies from the ground-state configuration $6s^1 4f^n$ to the excited-state configurations $6s^1 5d^1 4f^{n-1}$ and $5d^2 4f^{n-1}$.

bonds with hydrogen and oxygen atoms. On the other hand, since the closed-shell $6s^2$ configuration is nonbonding, a state with this configuration cannot be effective either for O–H activation. Thus, $5d^1 6s^1 4f^{n-1}$ is the most effective configuration compared with $6s^1 4f^n$, $6s^2 4f^{n-1}$, and $5d^2 4f^{n-1}$ for the insertion process.

4.3. The Comparison between Reactions of $\text{Ln}^+-(\text{CH}_3\text{OH})_n^+$ and $\text{LnO}^+-(\text{CH}_3\text{OH})_n^+$. The reaction of Ln^+ with methanol molecules can form $\text{Ln}^+-(\text{CH}_3\text{OH})_n^+$ at least in the initial stage, since ion–molecule association reactions are generally believed to proceed without an activation barrier.³¹ In this product, Ln^+ is expected to be bonded to the oxygen atom in the methanol molecule and the interaction is electrostatic in nature.³² The association product may be stabilized by evaporation of solvents or by collision with a third body such as He. However, if Ln^+ is very reactive, it may insert into the O–H bond of the methanol molecule to form an intermediate $\text{H–Ln}^+–\text{OCH}_3$. This intermediate undergoes a hydrogen-loss process to produce LnOCH_3^+ . In this product ion, Ln^+ is bonded to the oxygen atom and the bond may have a certain extent of covalent character. For the product LnCH_2O^+ , deuteration experiments have established that for the two lost hydrogen atoms, one comes from the OH group and another comes from the CH_3 group. Thus, the $\text{H–Ln}^+–\text{OCH}_3$ intermediate may undergo β -hydrogen transfer commonly observed in organometallic reaction (ref 15, 33) to form $\text{H(H)Ln}^+–\text{OCH}_2$. This leads to double dehydrogenations to give LnOCH_2^+ similar to the previously proposed mechanism for the reaction of Sc^+ and Y^+ with methanol molecules.¹² Since Ln^+ has two valence electrons, LnOCH_2^+ may have a structure in which Ln^+ is bonded to the oxygen and carbon atoms to form a triangle so that both the oxygen and the carbon fulfill the octet rule.

For larger clusters $\text{Ln}(\text{CH}_3\text{OH})_n^+$ ($n \geq 2$), the dehydrogenation products are $\text{Ln}(\text{OCH}_3)_2(\text{CH}_3\text{OH})_{n-2}^+$ or $\text{LnOCH}_2^+(\text{CH}_3\text{OH})_{n-1}^+$ cluster ions (except for Eu^+) with the loss of two hydrogen atoms. The deuterium-substitution experiment has excluded the latter structure. The reaction may still proceed through an insertion process like that for the reaction with single methanol molecules. However, it is not clear whether the double dehydrogenation occurs simultaneously or is a stepwise dehydrogenation process.

For the product ion $\text{Ln}(\text{OCH}_3)_2^+(\text{CH}_3\text{OH})_{n-2}$ (except Eu^+), the oxidation state of Ln^+ is expected to be close to +3, and it forms two covalent bonds with the two OCH_3^- groups. This is consistent with the fact that in the condensed phase the most stable oxidation state of the lanthanide element is +3. In product ions $\text{Ln}(\text{OCH}_3)_2^+(\text{CH}_3\text{OH})_{n-2}$, there are many electrostatic bonds between the central metal ion and the solvent methanol molecules in the cluster and the system is stabilized. The forces that drive the reaction are likely to be related to the relative thermodynamic stability of the reactant and the product. The situation here is found to be quite similar to that of the alkaline earth metal–methanol cluster ion systems. In particular, for Eu^+ , the dehydrogenation reaction occurs for $n \geq 5$ and the reaction product is $\text{EuOCH}_3^+(\text{CH}_3\text{OH})_{n-1}$. The reason only single dehydrogenation occurs is that in the product Eu has an oxidation state close to +2 similar to the alkaline earth metal ions that correspond to a $4f^7$ electronic configuration. The half-filled f orbitals make the Eu^{2+} much more stable than other oxidation state.

Lanthanide oxide cations LnO^+ such as LaO^+ were found to react with methanol clusters, leading to $\text{LnO}_2\text{C}_2\text{H}_6(\text{CH}_3\text{OH})_{n-2}^+$ with the loss of one water molecule. This type of reaction product was also observed by Azzaro et al. for the reactions of MO^+ ($\text{M} = \text{Sc}, \text{Y}, \text{and Lu}$) with methanol molecules. They proposed an intermediate $\text{CH}_3\text{O}-\text{M}^+-\text{OH}$ for the reaction mechanism.¹² The final product $\text{MO}_2\text{C}_2\text{H}_6^+$ was thought to have a dimethoxide–metal structure $\text{M}(\text{OCH}_3)_2^+$ on the basis of the energetic arguments. Our experiment is somewhat different in that the reaction is carried out between LnO^+ and methanol clusters instead of methanol molecules. Although $\text{M}(\text{OCH}_3)_2^+$ could well be the structure for the product, we cannot exclude other possibilities such as $\text{LaO}(\text{CH}_3\text{OCH}_3)(\text{CH}_3\text{OH})_{n-2}^+$ at present, especially when considering the very high bond dissociation energy for $\text{La}-\text{O}$ bond.^{20a}

5. Summary

We have studied the reactions between the 14 lanthanide cations (from La^+ to Lu^+ except Pm^+) and methanol clusters using a pick-up source and an RTOFMS. It was found that these lanthanide ions exhibit different reactivities toward methanol clusters. Those reactive ions including La^+ , Ce^+ , Pr^+ , Nd^+ , Gd^+ , Tb^+ , Ho^+ , Er^+ , and Lu^+ can react with methanol molecules to give dehydrogenation products such as LnCH_2O^+ and LnCH_3O^+ . For large clusters, the observed product ions are $\text{Ln}(\text{OCH}_3)_2^+(\text{CH}_3\text{OH})_{n-2}^+$. On the other hand, the relatively unreactive lanthanide ions including Sm^+ , Eu^+ , Dy^+ , Tm^+ , and Yb^+ cannot activate the $\text{O}-\text{H}$ bond during their collisions with the methanol molecules. It was found that only when they are solvated by a sufficient number of methanol molecules does the dehydrogenation reaction occur and give $\text{Ln}(\text{OCH}_3)_2^+(\text{CH}_3\text{OH})_{n-2}$ ($\text{LnOCH}_3^+(\text{CH}_3\text{OH})_{n-1}$ for Eu^+). It appears that the formation of the cluster ions, in which many methanol molecules are electrostatic-bonded to the central metal ions, renders the dehydrogenation reaction to readily occur even for the very unreactive metal ions.

The different reactivities of the lanthanide ions were found to be very sensitive to their electronic structures, which give rise to different promotion energies from their ground-state configurations with only one non- f valence electron (typically $6s^{14}f^n$) to the lowest-lying excited-state configuration with two non- f valence electrons (typically $6s^{15}d^14f^{n-1}$). The lower the promotion energy, the higher the reactivity of the lanthanide ion toward methanol molecules. The relationship between these two is consistent with an insertion mechanism for the reaction,

in which the Ln^+ needs two reactive valence electrons to form two covalent bonds with the oxygen and hydrogen atoms.

For the lanthanide–methanol cluster ion, the dehydrogenation reaction can be considered as the oxidation reaction of Ln^+ , in which Ln attains an oxidation state of +3 (+2 for Eu) in the reaction products such as $\text{Ln}(\text{OCH}_3)_2^+(\text{CH}_3\text{OH})_{n-2}$. These oxidation states, in fact, are the favorite oxidation states for lanthanide elements in the condensed phase. Thus, the rare earth metal ion–cluster reactions evolve from a gas-phase reaction type to a condensed reaction type at a cluster size containing only a few methanol molecules.

The reactions of LnO^+ with methanol clusters initially form the association products $\text{LnO}(\text{CH}_3\text{OH})_n^+$. These cluster ions can undergo a dehydration reaction resulting in $\text{LnO}_2\text{C}_2\text{H}_6(\text{CH}_3\text{OH})_{n-2}^+$, which have the same masses as those from the dehydrogenation reaction of $\text{Ln}(\text{CH}_3\text{OH})_n^+$. Besides, above a certain cluster size, the reaction of $\text{LnO}(\text{CH}_3\text{OH})_n^+$ to give $\text{LnO}_2\text{C}_2\text{H}_6(\text{CH}_3\text{OH})_{n-2}^+$ is quenched, and the association product series $\text{LnO}(\text{CH}_3\text{OH})_n^+$ reappears for n at around 13 for the lanthanide ions such as La^+ and Pr^+ .

Acknowledgment. The authors thank Qifei Wu and Rowenna Leung for their assistance in the experiments. This work is supported by a Grant from the Croucher Foundation (CF95/96.SC02). Financial support from an HIA program of HKUST is acknowledged.

References and Notes

- (1) *Industrial Applications of Rare Earth Elements*; Gschneider, K. A., Ed.; American Chemical Society: Washington, DC, 1981.
- (2) Schumann, H.; Genthe, W. In *Handbook on the Physics and Chemistry of Rare Earths*; Gschneider, K. A., Jr., Eyring, L., Eds.; North-Holland: New York, 1984; Vol. 7, p 445.
- (3) (a) Otsura, K.; Shimizu, Y.; Komatsu, T. *Chem. Lett.* **1987**, 9, 1835. (b) Watson, P. L.; Parshall, G. W. *Acc. Chem. Res.* **1985**, 18, 51. (c) Ashcroft, T.; Cheetham, A. K.; Foord, J. S.; Green, M. L. H.; Grey, C. P.; Murrell, A. J.; Vernon, P. D. F. *Nature* **1990**, 344, 319. (d) Capitan, M. J.; Malet, J.; Centeno, M. A.; Munoz-Paez, A.; Carrizosa, L.; Odriozola, J. A. *J. Phys. Chem.* **1993**, 97, 9223.
- (4) (a) Jeske, G.; Lauke, H.; Mauermann, H.; Swepston, P. N.; Schumann, H.; Marks, T. J. *J. Am. Chem. Soc.* **1985**, 107, 8091. (b) Jeske, G.; Schock, L. E.; Swepston, P. N.; Schumann, H.; Marks, T. J. *J. Am. Chem. Soc.* **1985**, 107, 8103. (c) Jeske, G.; Lauke, H.; Mauermann, H.; Schumann, H.; Marks, T. J. *J. Am. Chem. Soc.* **1985**, 107, 8111.
- (5) Bruzzzone, M.; Carbonaro, A. In *Fundamental and Technological Aspects of Organo-f-Element Chemistry*; Marks, T. J., Fragala, I. L., Eds.; D. Reidel Publishing Company: Boston, MA, 1984; p 387.
- (6) Molander, G. A. *Chem. Rev.* **1992**, 92, 29.
- (7) (a) Herrmann, W. A.; Anwender, R.; Denk, M. *Chem. Ber.* **1992**, 125, 2399. (b) Benelli, C.; Caneschi, D.; Gatteschi, D.; Sessoli, R. *Adv. Mater.* **1992**, 4, 504. (c) Barnhart, D. M.; Clark, D. L.; Huffman, J. C.; Vincent, R. L.; Watkin, J. G. *Inorg. Chem.* **1993**, 32, 4077. (d) Bradley, D. C.; Chudzynska, A.; Hurthhouse, M. B.; Motevalli, M.; Wu, R. *Polyhedron* **1994**, 13, 1.
- (8) Huang, Y.; Wise, M. B.; Jacobson, D. B.; Freiser, B. S. *Organometallics* **1987**, 6, 346.
- (9) Schilling, J. B.; Beauchamp, J. L. *J. Am. Chem. Soc.* **1988**, 110, 15.
- (10) Sunderlins, L. S.; Armentrout, P. B. *J. Am. Chem. Soc.* **1989**, 111, 3845.
- (11) Sunderlins, L. S.; Armentrout, P. B. *Organometallics* **1990**, 9, 1248.
- (12) Azzaro, M.; Breton, S.; Decouzon, M.; Geribaldi, S. *Int. J. Mass Spectrom. Ion Processes* **1993**, 128, 1.
- (13) Yin, W. W.; Marshall, A. G.; Marcalo, J.; de Matos, A. P. *J. Am. Chem. Soc.* **1994**, 116, 8666.
- (14) Heinemann, C.; Schroder, D.; Schwarz, H. *Chem. Ber.* **1994**, 127, 1807.
- (15) Cornehl, H. H.; Heinemann, C.; Schroder, D.; Schwarz, H. *Organometallics* **1995**, 14, 992.
- (16) Heinemann, C.; Goldberg, N.; Tornieporth-Oetting, I. C.; Klapotke, T. M.; Schwarz, H. *Angew. Chem., Int. Ed. Engl.* **1995**, 34, 213.
- (17) Geribaldi, S.; Breton, S.; Decouzon, M.; Azzaro, M. *J. Am. Chem. Soc.* **1996**, 118, 1151.
- (18) Cornehl, H. H.; Hornung, G.; Schwarz, H. *J. Am. Chem. Soc.* **1996**, 118, 9960.

- (19) Gibson, J. K. *J. Phys. Chem.* **1996**, *100*, 15688.
- (20) (a) Lu, W. Y.; Huang, R. B.; Yang, S. H. *J. Phys. Chem.* **1995**, *99*, 12099. (b) Lu, W. Y.; Yang, S. H. *J. Phys. Chem. A* **1998**, *102*, 825.
- (21) Chandrasekharaiah, M. S.; Gingerich, K. A. In *Handbook on the Physics and Chemistry of Rare Earths*; Gschneidner, K. A., Jr., Eyring, L., Eds.; North-Holland: New York, 1989; Vol. 12, p 409.
- (22) *CRC Handbook of Chemistry and Physics*, 77th ed.; Lide, D. R., Ed.; CRC Press: London, 1996.
- (23) (a) Selegue, T. J.; Lisy, J. M. *J. Am. Chem. Soc.* **1994**, *116*, 4874. (b) Lu, W. Y.; Yang, S. H. *Int. J. Mass Spectrom. Ion Processes*, in press.
- (24) Draves, J. A.; Lisy, J. M. *J. Am. Chem. Soc.* **1992**, *112*, 9006.
- (25) Zhang, X.; Castleman, Jr., A. W. *J. Am. Chem. Soc.* **1992**, *114*, 8607.
- (26) Shirota, H.; Pal, H.; Tominaga, K.; Yoshihara, K. *J. Phys. Chem.* **1996**, *100*, 14575.
- (27) J. E. Huheey, E. A. Keiter, R. L. Keiter, *Inorganic Chemistry: Principles of Structure and Reactivity*, 4th ed.; HarperCollins College Publishers: New York, 1993; p 604.
- (28) Weisshaar, J. C. *Acc. Chem. Res.* **1993**, *26*, 213.
- (29) Martin, W. C.; Zalubas, R.; Hagan, L. *Atomic Energy Levels—The Rare Earth Elements*; National Bureau of Standards: Washington, DC, 1978.
- (30) Goldschmidt, Z. B. In *Handbook on the Physics and Chemistry of Rare Earths*; Gschneidner, K. A., Jr., Eyring, L., Eds.; North-Holland: New York, 1978; Vol. 1, p 88.
- (31) Magnera, T. F.; David, D. E.; Stulik, D.; Orth, R. G.; Jonkman, H. T.; Michl, J. *J. Am. Chem. Soc.* **1989**, *111*, 5036.
- (32) Rosi, M.; Bauschlicher, C. W., Jr., *Chem. Phys. Lett.* **1990**, *166*, 189.
- (33) Eller, K. In *Organometallic Ion Chemistry*; Freiser, B. S., Ed.; Kluwer Academic Publishers: London, 1996; p 123.